MECSOL 2022 - Proceedings of the 8th International Symposium on Solid Mechanics
M.L. Bittencourt, J. Labaki, L.C.M. Vieira Jr. and E. Mesquita (Editors), Campinas SP, Brazil, October 17th to 19th, 2022

MECSOL 2022 – Complex Band Structure of Flexural Waves in Thin Platonic Crystals

E.J.P. Miranda Jr.[1-3], V.F. Dal Poggetto[4], N.M. Pugno[4,5], J.M.C. Dos Santos[3]

[1] Federal Institute of Maranhão, IFMA-EIB-DE, Rua Afonso Pena, 174, CEP 65010-030, São Luís, MA, Brazil
[2] Federal Institute of Maranhão, IFMA-PPGEM, Avenida Getúlio Vargas, 4, CEP 65030-005, São Luís, MA, Brazil
[3] University of Campinas, UNICAMP-FEM-DMC, Rua Mendeleyev, 200, CEP 13083-970, Campinas, SP, Brazil
[4] Laboratory for Bio-inspired, Bionic, Nano, Meta Materials & Mechanics, Department of Civil, Environmental and Mechanical Engineering, University of Trento, 38123 Trento, Italy
[5] School of Engineering and Materials Science, Queen Mary University of London, Mile End Road, London E1 4NS, United Kingdom

Abstract. The flexural wave propagation in a 2-D platonic crystal with periodic arrays of inclusions in square and honeycomb lattices is investigated. This platonic crystal is capable of filtering the propagation of flexural waves over a specified range of frequency due to the formation of Bragg-type band gaps. The band structures are obtained by the improved plane wave expansion (IPWE) and extended plane wave expansion (EPWE) considering the Kirchhoff-Love thin plate theory. The band gaps are opened up with different values of unit cell wave attenuation. The type of lattice influences significantly the propagating and the evanescent modes. The presented results can be used to investigate the elastic wave attenuation using 2-D platonic periodic structures.
Keywords: periodicity, band gaps, wave attenuation, evanescent waves

INTRODUCTION

Plate structures are widely used in aeronautical, mechanical and civil engineering, aerospace, manufacturing etc. They are one of the most commonly used structural components (Li et al., 2019). In this context, the phononic crystal (PnC) plates, also known as platonic crystals, have been widely used for vibration reduction (Jung *et al.*, 2020).

PnCs are artificial composite structures composed of units arranged in a specific spatially periodic form. By designing the material composition and/or spatial arrangement of the artificial unit cell, PnCs can exhibit unusual dispersion characteristics (Hu *et al.*, 2021) able to manipulate the distribution and propagation of mechanical waves. PnCs have been also applied to vibration attenuation, as mechanical wave filters, seismic wave shields, acoustic barriers, noise suppression devices, among others (Miniaci *et al.*, 2016; Miniaci *et al.*, 2018; Dal Poggetto *et al.*, 2021). The most common strategy to analyse the wave attenuation behaviour in a PnC is to compute its complex band structure (Miranda Jr. *et al.*, 2022).

The main purpose of this investigation is to study the complex band structure of a 2-D thin platonic crystal composed by circular inclusions in a matrix with square and honeycomb lattices assuming flexural wave propagation and the Kirchhoff-Love thin plate theory (Kirchhoff, 1850; Love, 1888).

SIMULATED EXAMPLES

The improved plane wave expansion (IPWE), $\omega(\mathbf{k})$ approach, and the extended plane wave expansion (EPWE), $\mathbf{k}(\omega)$ approach, are commonly used, respectively, to compute the propagating and evanescent modes of the band structure, where $\mathbf{k}$ is the Bloch wave vector and ω is the angular frequency. The formulations are not derived for brevity. Moreover, the IPWE formulation has already been derived in many preceding works, justifying its use and effect in improving the convergence of the method (Sigalas and Economou, 1994; Yao *et al.*, 2009; Li, 1996; Cao *et al.*, 2004). The Kirchhoff-Love thin plate theory (Kirchhoff, 1850; Love, 1888) can be used to model 2-D platonic crystals with periodic arrays of circular inclusions in square and honeycomb lattices. The nomenclature of "honeycomb" lattice is based on previous studies (Torrent *et al.*, 2013).

Figure 1 sketches the transverse cross sections of the 2-D platonic crystal with square (a) and honeycomb (b) lattices. In Fig. 1, it is also shown the first irreducible Brillouin zone (FIBZ) (Brillouin, 1946) of the 2-D platonic crystal for square (c) and honeycomb (d) lattices, where the FIBZ high-symmetry points are $\Gamma\ (0,0)$, X $(\pi/a,0)$ and M $(\pi/a,\pi/a)$ for the square lattice and $\Gamma\ (0,0)$, X $(4\pi/3\sqrt{3}a,0)$ and M $(\pi/\sqrt{3}a,\pi/3a)$ for the honeycomb lattice, where a is the lattice parameter.

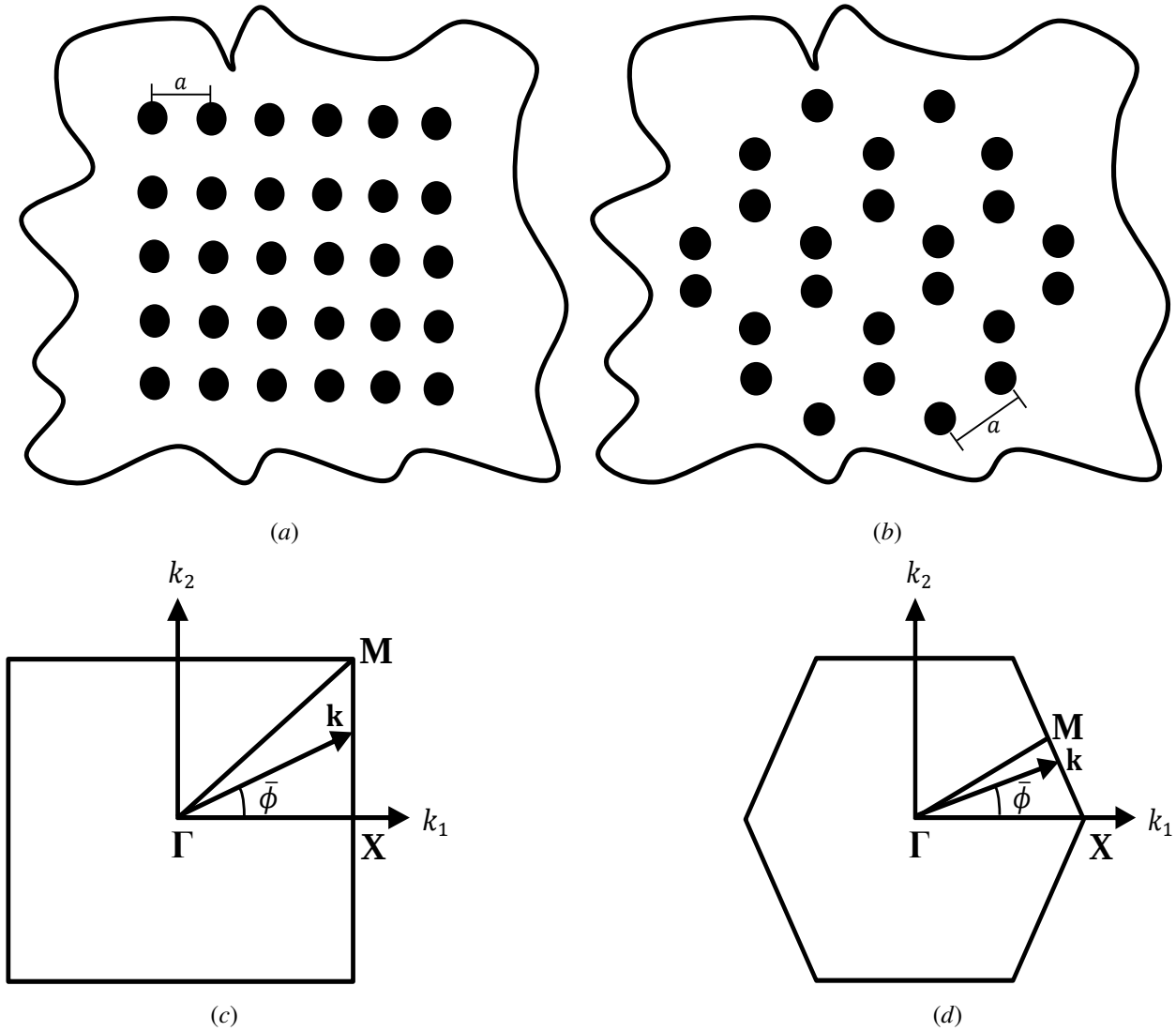

Figure 1 – Transverse cross sections of the 2-D platonic crystal with circular inclusions in a square (a) and honeycomb (b) lattices, and the FIBZ for square (c) and honeycomb (d) lattices.

The physical parameters (Yao *et al.*, 2009) of Al_2O_3 circular inclusions (A) and Epoxy matrix (B) of the 2-D platonic crystals are listed in Tab. 1. The lattice parameter is considerable huge ($a = 22$ m), in order to shift the band gaps (Bragg-type) to lower frequencies when using EPWE for reducing the computing cost. Thus, using the reduced frequency to plot the band structure ($\Omega = \omega a/2\pi C_{t_B}$), where $C_{t_B} \approx 1.1756 \times 10^3$ m/s is the transverse velocity in the matrix, Bragg-scattering band gaps opened up for a unit cell with lattice parameter of 22 mm, 22 cm and 22 m are the same, for instance. Moreover, it is only considered the complete and partial (along ΓX direction) band gaps until $\Omega = 1$. For a better understanding of the following results, the basic issues of real and complex 2-D band structures can be revised in Kushwaha *et al.* (1993) and Laude *et al.* (2009).

For EPWE calculations, the model assurance criterion (MAC) (Mencik, 2010) is used to estimate the correlation among wave shapes. The band structures computed by the IPWE approach regarded 49 and 441 plane waves. Next, for IPWE/EPWE calculation and comparison, 49 plane waves are considered, in order to reduce the computational time.

Figures 2 and 3 illustrate the propagating part of the band structure of the 2-D platonic crystal regarding 49 (a) and 441 (b) plane waves, computed by the IPWE, for square and honeycomb lattices, respectively. The complete and partial (along the ΓX direction) band gaps are represented using shaded regions. For the square lattice (Fig. 2), one complete and two partial band gaps along the ΓX direction are observed. In Fig. 3 (honeycomb lattice), there are two complete and

Table 1 – Geometry and material properties of the Al_2O_3 circular inclusions (A) and Epoxy matrix (B) (Yao *et al.*, 2009).

Geometry/Property	Value
Lattice parameter (a)	22 m
Filling fraction ($\bar{f}$)	0.283
Mass density (ρ_A, ρ_B)	3.97×10^3 kg/m^3, 1.142×10^3 kg/m^3
Young's modulus (E_A, E_B)	402.7×10^9 N/m^2, 4.35×10^9 N/m^2
Poisson's ratio (ν_A, ν_B)	0.23, 0.378

many (b) partial band gaps.

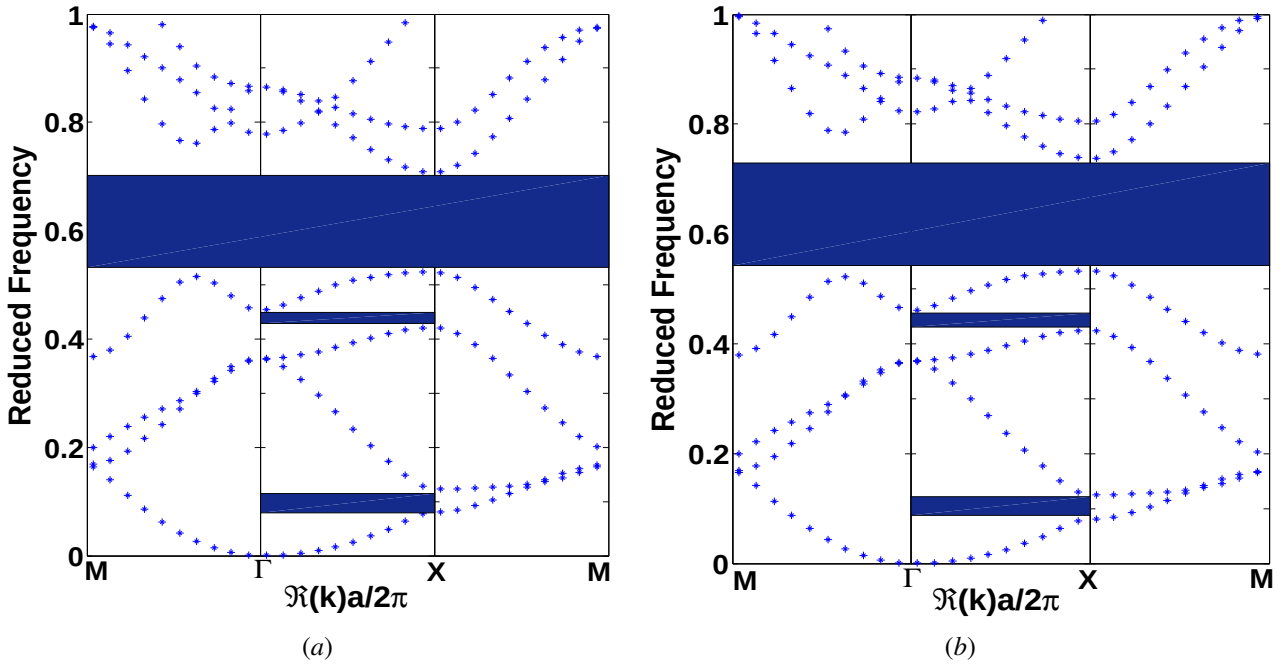

Figure 2 – Band structures of the 2-D platonic crystal with square lattice and circular inclusions for 49 (a) and 441 (b) plane waves. The complete and partial (along ΓX direction) band gaps are identified by the shaded regions.

Moreover, for the honeycomb lattice, there are some partial band gaps along ΓX direction that are not opened up (a) when using only 49 plane waves. For the honeycomb lattice, it can be observed that more band gaps are opened up, even though they are narrower than for square lattice (Fig. 2). Furthermore, more wave modes exist for the honeycomb lattice (Fig. 3), thus the convergence is poor for this lattice, which should be associated with the fact that the unit cell of a honeycomb lattice has two inclusions. The influence of lattice type on the band structure (considering only the real part of Bloch wave vector, *i.e.*, purely propagating waves) has already been discussed for solid PnCs (Miranda Jr. and Dos Santos, 2017).

In Fig. 4, the comparison of the band structure computed by IPWE using 49 (red circles) and 441 (blue asterisks) plane waves for square (a) and honeycomb (b) lattices is illustrated. It can be observed that the modes present good agreement for both lattices regarding lower frequencies. However, for higher frequencies, there are a significant mismatching. Nevertheless, the next results are computed with 49 planes just for computational cost reduction.

In Figs. 5 and 6, the complex band structures for square and honeycomb lattices, respectively, along ΓX direction, *i.e.*, $\bar{\phi} = 0$, is shown. The wave modes in the complex band structures can be purely real (propagating), purely imaginary (evanescent) or complex (evanescent). The real part of the reduced Bloch wave vector ($\mathbf{k}a/2\pi$) is illustrated in Figs. 5 and 6 (a) and it is computed by both the IPWE (blue circles) and EPWE (coloured points) approaches.

A good agreement between the IPWE and EPWE methods is observed in Figs. 5 and 6 (a). However, some modes captured by the EPWE method are not obtained by the IPWE in Figs. 5 and 6 (a), since these modes are complex and IPWE only identifies purely propagating (real) modes (Laude *et al.*, 2009). Hereafter, the band gaps identified in Figs. 2 and 3 (a) are illustrated by using coloured dashed lines.

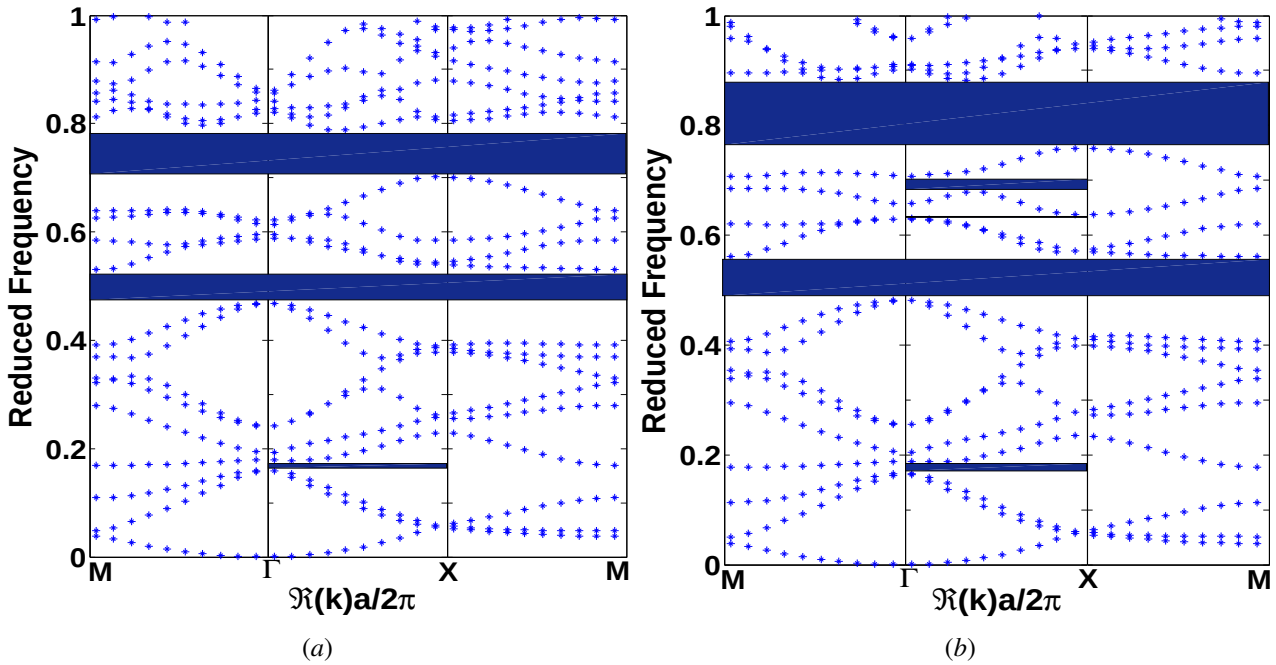

Figure 3 – Band structures of the 2-D platonic crystal with honeycomb lattice and circular inclusions for 49 (a) and 441 (b) plane waves. The complete and partial (along ΓX direction) band gaps are identified by the shaded regions.

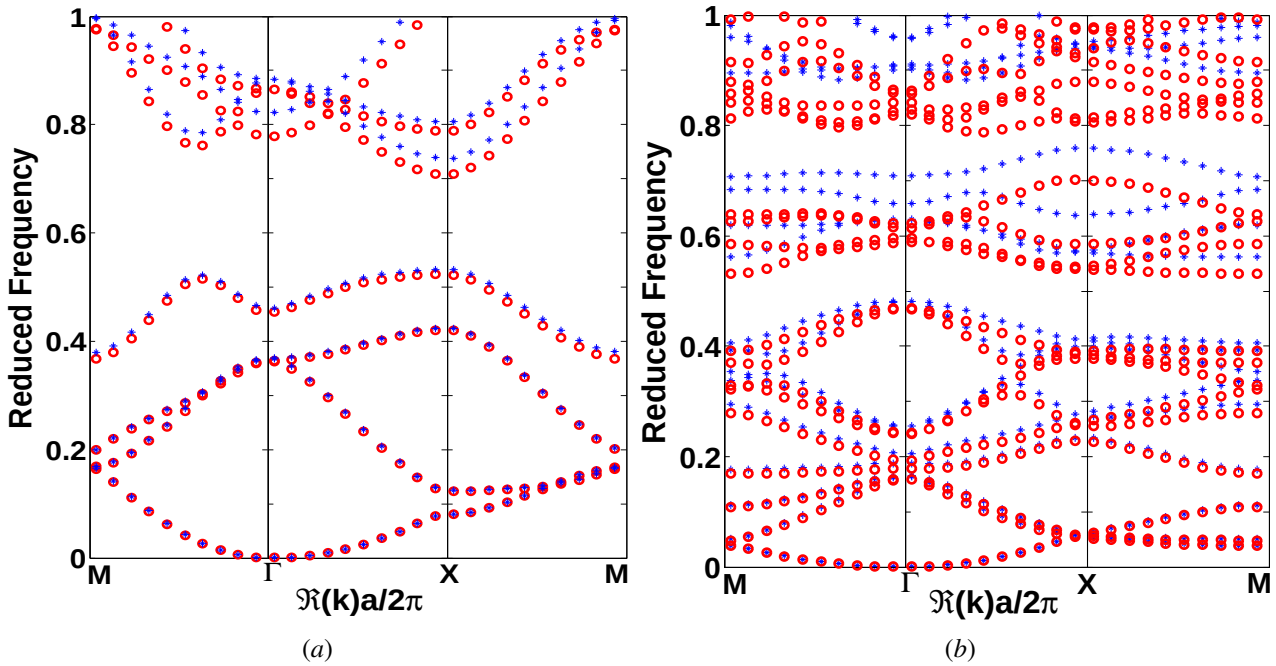

Figure 4 – Band structure comparison of the 2-D platonic crystals with square (a) and honeycomb (b) lattices, considering 49 (red circles) and 441 (blue asterisks) plane waves.

In Fig. 7, only the smallest positive imaginary part (least attenuated wave mode) of the reduced Bloch wave vector (lowest component whose real part of the reduced Bloch wave vector lies inside and around the FIBZ is the most accurate (Miranda Jr. and Dos Santos, 2019)) are plotted for the square (a) and honeycomb (b) lattices.

Figures 8 and 9 show the complex band structure (positive and negative values) for square and honeycomb lattices, respectively, along the ΓX direction, computed by the (a) IPWE (blue circles) and $(a-b)$ EPWE (coloured points)

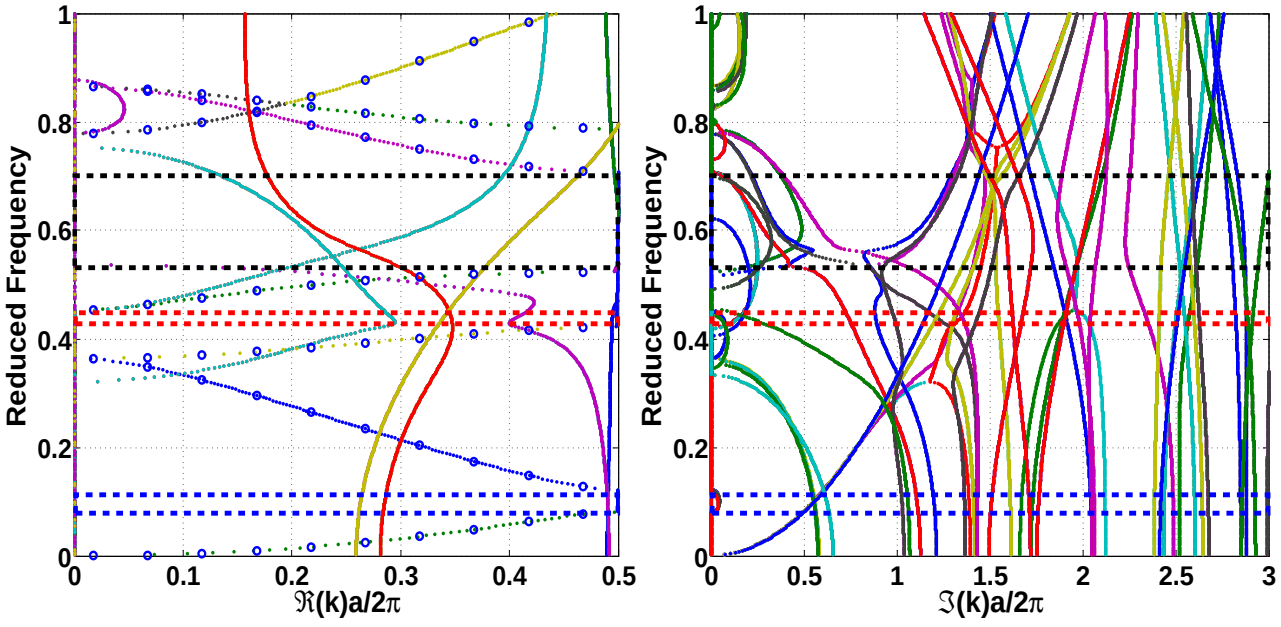

(*a*) (*b*)

Figure 5 – Complex band structure (along the ΓX direction) of the 2-D platonic crystal with square lattice and circular inclusions computed by (a) IPWE (blue circles) and $(a-b)$ EPWE (coloured points) approaches. The complete and partial band gaps are identified by the coloured dashed lines.

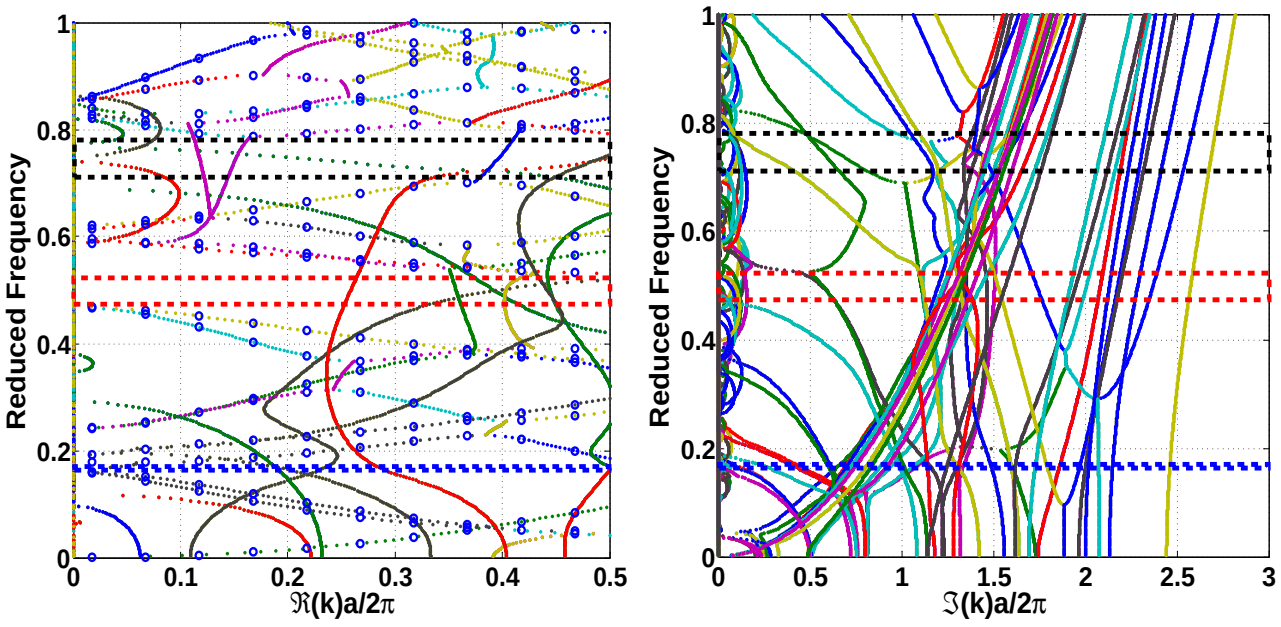

(*a*) (*b*)

Figure 6 – Complex band structure (along the ΓX direction) of the 2-D platonic crystal with honeycomb lattice and circular inclusions computed by (a) IPWE (blue circles) and $(a-b)$ EPWE (coloured points) approaches. The complete and partial band gaps are identified by the coloured dashed lines.

approaches, considering only the complex modes (computed by EPWE) which match the real modes (computed by IPWE) along ΓX direction.

From Figs. 8 and 9, it can be observed that the modes obtained by EPWE (those that agree with the PWE) present a

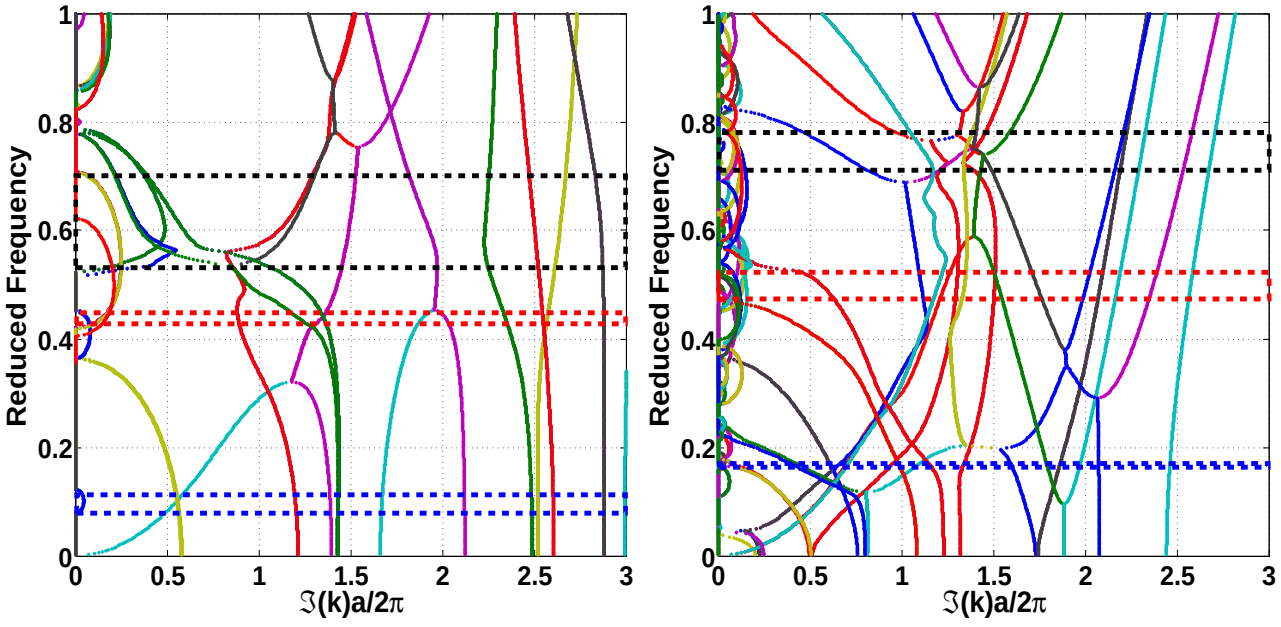

(*a*) (*b*)

Figure 7 – Lowest imaginary part of the complex band structure (along the ΓX direction) of the 2-D platonic crystal with square (a) and honeycomb (b) lattices with circular inclusions computed by EPWE. The complete and partial band gaps are identified by the coloured dashed lines.

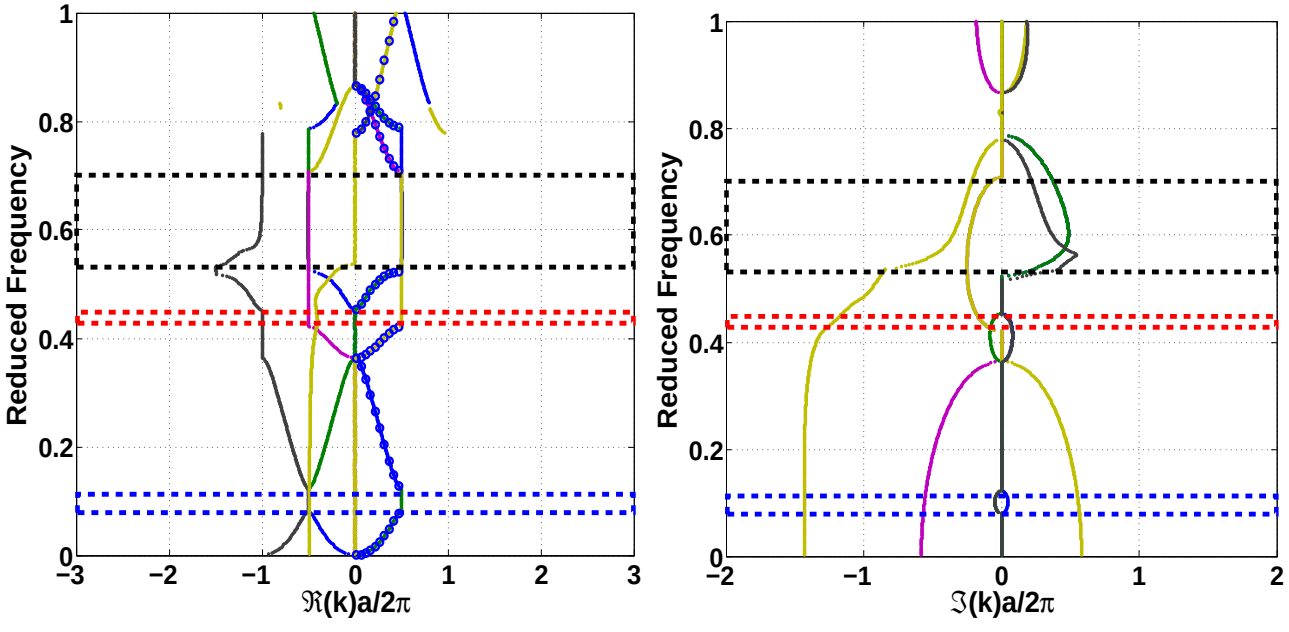

(*a*) (*b*)

Figure 8 – Complex band structure (along the ΓX direction) of the 2-D platonic crystal with square lattice and circular inclusions computed by (a) IPWE (blue circles) and $(a-b)$ EPWE (coloured points) approaches, considering only the complex modes (computed by EPWE) which match the real modes (computed by IPWE). The complete and partial band gaps are identified by the coloured dashed lines.

complex pattern and are nonsymmetrical.

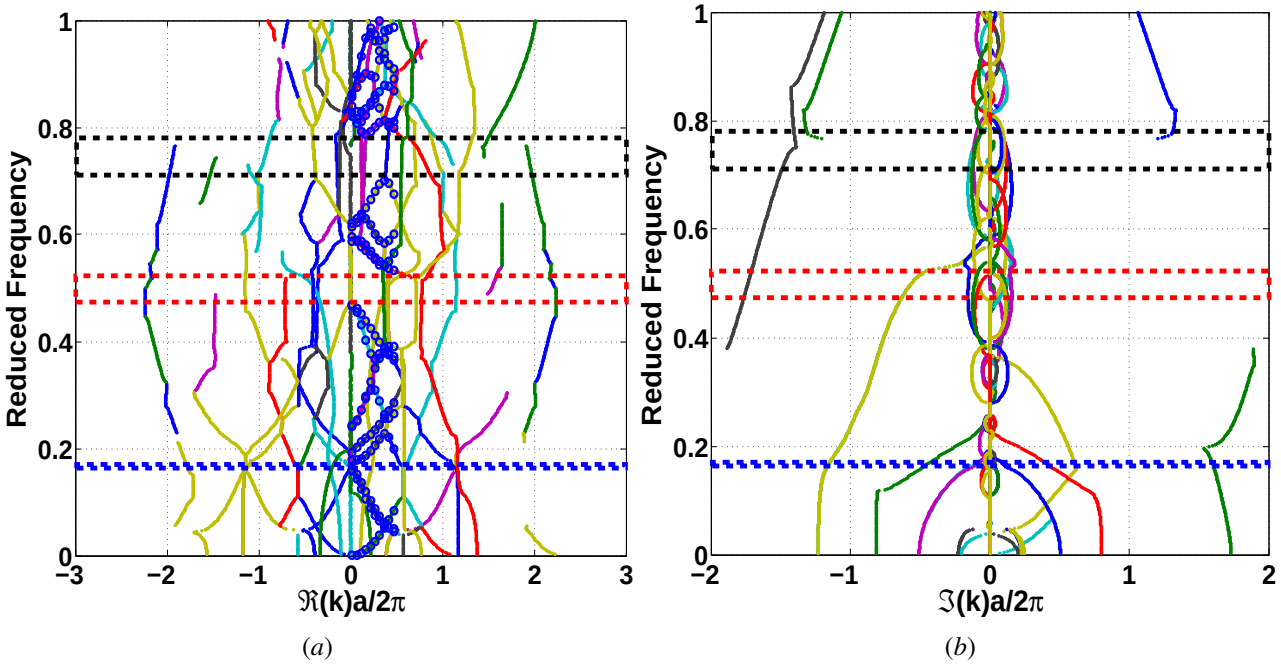

Figure 9 – Complex band structure (along the ΓX direction) of the 2-D platonic crystal with honeycomb lattice and circular inclusions computed by (a) IPWE (blue circles) and $(a-b)$ EPWE (coloured points) approaches, considering only the complex modes (computed by EPWE) which match the real modes (computed by IPWE). The complete and partial band gaps are identified by the coloured dashed lines.

CONCLUSIONS

The complex band structure of a 2-D platonic crystal with circular inclusions in square and honeycomb lattices is computed considering the IPWE and EPWE approaches to obtain the propagating and evanescent modes, respectively.

First, the band structure is investigated by the IPWE considering only flexural propagating waves. Next, the flexural evanescent waves are also obtained using the EPWE. Some complex modes cannot be computed by the IPWE. The 2-D platonic crystal with honeycomb lattice opens up more complete and partial (along ΓX direction) Bragg-type band gaps.

ACKNOWLEDGMENTS

EJPM and JMCS thank the Brazilian funding agencies CAPES (finance Code 001), CNPq (grants 313620/2018, 151311/2020-0 and 403234/2021-2), FAPEMA (grants 02558/21, 02559/21 and 00680/22), and FAPESP (grant 2018/15894-0).

REFERENCES

Brillouin, L., 1946, "Wave Propagation in Periodic Structures", Dover Publications, New York.

Cao, Y., Hou, Z., Liu, Y., 2004, "Convergence Problem of Plane-Wave Expansion Method for Phononic Crystals", Phys. Lett. A, Vol. 327, No. 2-3, pp. 247-253.

Dal Poggetto, V.F., Bosia, F., Miniaci, M., Pugno, N.M., 2021, "Band Gap Enhancement in Periodic Frames Using Hierarchical Structures", Int. J. Solids Struct., Vol. 216, pp. 68-82.

Hu, W., Ren, Z., Wan, Z., Qi, D., Cao, X., Li, Z., Wu, W., Tao, R., Li, Y., 2021, "Deformation Behavior and Band Gap Switching Function of 4D Printed Multi-Stable Metamaterials", Mater. Des., Vol. 200, pp. 109481.

Jung, J., Goo, S., Kook, J., 2021, "Design of a Local Resonator Using Topology Optimization to Tailor Bandgaps in Plate Structures", Mater. Des., Vol. 191, pp. 108627.

Kirchhoff, G., 1850, "Über das Gleichgewicht und die Bewegung einer elastischen Scheibe", J. Reine Angew. Math., Vol. 40, pp. 51–88.

Kushwaha, M.S., Halevi, P., Dobrzynski, L., Djafari-Rouhani, B., 1993, "Acoustic Band Structure of Periodic Elastic Composites", Phys. Rev. Lett. , Vol. 71, No. 13, pp. 2022-2025.

Laude, V., Achaoui, Y., Benchabane, S., Khelif, A., 2009, "Evanescent Bloch Waves and the Complex Band Structure of Phononic Crystals", Phys. Rev. B Condens. Matter, Vol. 80, No. 9, pp. 092301.

Li, L., 1996, "Use of Fourier Series in the Analysis of Discontinuous Periodic Structures", J. Opt. Soc. Am. A, Vol. 13, No. 9, pp. 1870-1876.

Li, S., Dou, Y., Chen, T., Wan, Z., Huang, J., Li, B., Zhang, F., 2019, "Evidence for Complete Low-Frequency Vibration Band Gaps in a Thick Elastic Steel Metamaterial Plate", Mod. Phys. Lett. B, Vol. 33, No. 04, pp. 1950038.

Love, A.E.H., 1888, "The Small Free Vibrations and Deformation of a Thin Elastic Shell", Philos. Trans. R. Soc., Vol. 179, pp. 491–546.

Mencik, J.-M., 2022, "On the Low- and Mid-Frequency Forced Response of Elastic Structures using Wave Finite Elements with One-Dimensional Propagation", Comput. Struct., Vol. 88, pp. 674-689.

Miniaci, M., Krushynska, A., Bosia, F., Pugno, N.M., 2016, "Large Scale Mechanical Metamaterials as Seismic Shields", New J. Phys., Vol. 18, No. 8, pp. 083041.

Miniaci, M., Krushynska, A., Gliozzi, A.S., Kherraz, N., Bosia, F., Pugno, N.M., 2018, "Design and Fabrication of Bioinspired Hierarchical Dissipative Elastic Metamaterials", Phys. Rev. Appl., Vol. 10, No. 2, pp. 024012.

Miranda Jr., E.J.P., Rodrigues, S.F., Aranas Jr., C., Dos Santos, J.M.C., 2022, "Plane Wave Expansion and Extended Plane Wave Expansion Formulations for Mindlin-Reissner Elastic Metamaterial Thick Plates", J. Math. Anal. Appl., Vol. 505, pp. 125503.

Miranda Jr., E.J.P., Dos Santos, J.M.C., 2017, "Band Structure in Carbon Nanostructure Phononic Crystals", Mater. Res.-Ibero-Am. J., Vol. 20, Suppl. 2, pp. 555-571.

Miranda Jr., E.J.P., Dos Santos, J.M.C., 2019, "Flexural Wwave Band Gaps in Multi-Resonator Elastic Metamaterial Timoshenko Beams", Wave Motion, Vol. 91, Suppl. 2, pp. 102391.

Sigalas, M.M., Economou, E.N., 1994, "Elastic Waves in Plates with Periodically Placed Inclusions", J. Appl. Phys., Vol. 75, No. 6, pp. 2845-2850.

Torrent, D., Mayou, D., Sánchez-Dehesa, J., 2013, "Elastic Analog of Graphene: Dirac Cones and Edge States for Flexural Waves in Thin Plates", Phys. Rev. B Condens. Matter, Vol. 87, No. 6, pp. 115143.

Yao, Z.-J., Yu, G.-L., Wang, Y.-S., Shi, Z.-F., 2009, "Propagation of Bending Waves in Phononic Crystal Thin Plates with a Point Defect", Int. J. Solids Struct., Vol. 46, pp. 2571-2576.

RESPONSIBILITY NOTICE

The authors are the only parties responsible for the printed material included in this paper.